Nano-encapsulated PCM emulsions prepared by a solvent-assisted method for solar applications

Filippo Agresti [1], Laura Fedele [2], Stefano Rossi [2], David Cabaleiro [2,3], Sergio Bobbo [2], Gloria Ischia [4], Simona Barison [1,*]

[1] *CNR ICMATE, Corso Stati Uniti 4, 35127 Padova, Italy*

[2] *CNR ITC, Corso Stati Uniti 4, 35127 Padova, Italy*

[3] *Departamento de Física Aplicada, Facultade de Ciencias, Universidade de Vigo, 36310 Vigo, Spain*

[4] *Dipartimento di Ing. Industriale, Università degli studi di Trento, Via Sommarive 9, 38123 Trento, Italy*

Keywords: PCM emulsion, paraffin, nano-encapsulation, thermal properties, optical properties

Abstract

Phase change material emulsions (PCMEs) were largely investigated as potential working fluids for various applications as in HVAC systems, solar thermal storage, and heat transfer. They basically contain water and phase change materials, possess much larger energy storage capacity than currently used chilled water based systems and exploit higher thermal conductivity than bulk PCM reservoirs. Main barriers to their application are the difficulty in maintaining emulsion stability and the undercooling effect. In this work, a new solvent-assisted route was developed to produce nano-emulsions of commercial paraffin waxes in water. Concentrations from 2 to 10 wt% were obtained starting from two commercial paraffin waxes, with nominal melting temperatures around 55°C and 70°C. The droplet dimensions were verified and resulted below 100 nm for lower concentrations and slightly higher for 10 wt%. The stability of emulsions was verified by long-term tests. An undercooling effect was verified and strongly reduced by testing some nucleating agents. The heat of melting was lower than expected, probably due to PCM molecules on the surface of the nanoparticles anchored to the surfactant. However, calculating the thermal capacity of PCMEs with respect to pure water, a gain up to 40% for operating temperatures close to PCM melting temperature was estimated. Optical properties of single wall carbon nanohorns/paraffin composites were also measured.

* Corresponding author: simona.barison@cnr.it

1. Introduction

Heating and cooling in European buildings and industry account for half of the EU's energy consumption and for about 68% of its natural gas imports for EU households [1], and heating and hot water alone are responsible for 79% of total energy use [2]. Phase change material emulsions (PCMEs) or phase change slurries were largely investigated in the last years as potential working fluids which could be used to reduce energy consumption in HVAC systems [3]. They basically contain water and phase change materials (PCMs) and as such do possess much larger energy storage capacity than currently used chilled water based systems and exploit higher thermal conductivity than bulk PCM reservoirs. Emulsions or nano-encapsulated PCMs are pumpable and offer the advantage of higher heat transfer due to the presence of water phase and higher area/volume ratio of PCM phase. Besides HVAC, the applications and the temperature ranges investigated so far include solar thermal storage (where various temperatures ranges between 30 and 100°C were tested) [4], waste heat recovery and heat transfer (typically around 20, 50 or 60-65°C), intelligent building (where PCM were tested for various applications between 0 and about 90°C), etc. [5,6,7].

The main barrier to the application of PCME is the difficulty in maintaining stability in emulsions without experiencing temperature stratification during the phase change process. This led most of the researchers to study various types of PCM micro- or nano-encapsulation methods [8]. The undercooling, that is the emulsion cooling below its melting point without crystallization, is another typical issue of PCMEs as this phenomenon enlarges the operating temperature range of the systems, thus worsening the energy efficiency and coefficient of performance. Several papers were published trying to face these issue [9] but, even though there are few practical examples at industrial level of their use, yet still some critical problems need to be overcome before a competitive edge over actual systems can be achieved. As to the emulsion stability, various papers investigated strategies to improve it, as by micro-encapsulation methods [10], or by properly selecting emulsifiers and emulsification conditions [3,11,12,13]. Also the undercooling was widely investigated so far and various approaches to reduce it were proposed. In general, droplet sizes and their distribution have a significant influence on both melting and nucleation temperature. Both temperatures typically decrease with reducing droplet size [9]. Gunther et al. [14] tried to interpret the cause of undercooling with nucleation theory, which describes the formation of small particles of the new phase in the middle of the fluid phase. They observed that both deactivation and creation of nucleation sites have to be expected when dividing a PCM volume into small droplets. They supposed that nucleation rate in small droplets could be dominated by homogeneous nucleation, which again depends on the droplet size. It was also demonstrated that the surfactant has a strong impact on the process of nucleation. The use of nucleating agents, namely materials that act as seeds or catalysts for the heterogeneous nucleation and crystal growth, was widely adopted as an effective solution to reduce undercooling. The nucleating agent type and its content have important effects on both the melting and nucleation temperatures. With increasing fraction of the nucleating agent, the melting temperature of the PCM droplets decreases, but the nucleation temperature increases [9]. Various nucleating agents have been studied so far including e.g. multi-wall carbon nanotubes [15], even though for paraffin emulsions typically the papers report on the use of a small concentration of paraffin with higher melting point as nucleating agent [3,9,10].

In the field of solar collectors, the new tendency for employing PCMs as an energy storage system was investigated in several solar collectors [12]. PCM modules in water thermal energy storage tanks, or directly as heat sink integrated in the solar device, resulted promising in harvesting hot water at almost constant temperature during the shut-off of the energy supply [4,16]. These systems offer several advantages including high storage capacity, low storage volume, and isothermal operation during the charging and discharging processes. The integration of the PCM inside the flat-plate solar collectors showed a significant improvement in the collector efficiency and system cost reduction. However, to date there are no studies

on the integration of PCMs into a fluid that could directly absorb the solar radiation and convert it into latent heat, thus allowing direct storage of energy. In fact, some nanofluids based on water or glycol and containing carbon nanoparticles were proposed as fluids for volumetric absorption of solar radiation, to improve the efficiency of solar collectors [17,18]. The studies showed the feasibility of using nanofluid containing carbon nanostructures to efficiently absorb solar radiation even at very low concentrations of micro- or nano-particles. Since then, numerous studies have been proposed in this field, in which different types of fluids and nanoparticles, aside from various testing facilities, were studied [19,20]. The integration of carbon nanostructures with PCM in water could have the double function of using carbon nanostructure to both reduce undercooling and capture the solar radiation.

Typical methods to produce PCMEs include high-energy emulsification processes or low energy methods as phase inversion [3]. In this work, a new solvent-assisted route was developed to produce nano-emulsions of commercial paraffin waxes in water. Concentrations from 2 to 10 wt% were obtained starting from two commercial paraffin waxes, with nominal melting temperatures of 55°C and 70°C, respectively. The paraffin particle dimensions were verified by transmission electron microscopy (TEM). Particle size distribution and stability of emulsions were verified by Dynamic Light Scattering (DLS) and ζ-potential through long-term tests, mechanical stress experiments and freeze-taw cycles. Melting and crystallization temperatures as well as enthalpy of fusion were measured by differential scanning calorimetry (DSC). The thermal diffusivity of emulsions was also measured.

Two nucleating agents were investigated to reduce undercooling issue: a small concentration of the paraffin melting at 70°C in the paraffin melting at 55°C and a carbon nanostructure, namely single wall carbon nanohorns (SWCNHs). The choice of investigating a carbon/PCM composite was also driven by the interest in testing these emulsions as radiation absorber fluids for solar collectors. With this view, optical measurements were also performed to study the optical absorption of C/PCMEs.

2. Materials and methods

In this work, nano-emulsions of paraffin waxes in water were produced at PCM concentrations of 2, 4 and 10 wt% by a solvent-assisted route. PCMEs were prepared starting from two paraffin waxes, namely RT55 and RT70HC, commercialized by Rubitherm Technologies GmbH. According to the supplier, RT55 exhibits a melting temperature of 55°C and a melting heat of 170 kJ/kg (including both latent and sensible heat of fusion), while for RT70HC these values are 70°C and 260 kJ/kg, respectively.

The procedure consists in the preparation of two solutions, one of PCM into hexane (>98.5%, mixture of isomers, Sigma Aldrich) and one of sodium dodecyl sulphate (SDS) (98%, provided by Sigma Aldrich) in deionised water (Millipore, Billerica MA, USA, 18.2 MΩ·cm). Various surfactants were tested as emulsifiers (SDS, Triton X-100, cetyl trimethylammonium bromide, sodium docusate), but SDS gave the best results in terms of smaller particle size and emulsion stability over time and freeze-thaw cycles. A SDS:PCM=1:8 mass ratio was identified as the optimal value to achieve stable emulsions. The two solutions were placed into the same sonication bath (CEIA CP104 ultrasonic bath, 39 Hz, 100 W) at temperatures indicated in Table 1 for 30 min in order to uniform the temperature and to favour the dissolution of the PCM into hexane. The two solutions were then mixed together and sonicated in the CEIA CP104 ultrasonic bath for 5 min while shaking to obtain a stable emulsion. Then, they were further sonicated for 10 min using a Sonics VCX130 (Sonics & Materials, Inc.) operating at 20 kHz and 65 W, equipped with a 12 mm diameter Ti_6Al_4V alloy tip. The emulsions were then heated at 90°C and stirred to remove the hexane and to obtain bare nano-encapsulated paraffin emulsion in water. The evaporated water was reintegrated continuously after heating and the proper amount was eventually added to obtain the desired PCM concentration. The preparation parameters for each sample are summarized in table 1.

In order to investigate the effect of nucleation agents on the thermal behaviour of some nano-emulsions, two nucleating agents were tested. Firstly, two emulsions were formulated using the same preparation route as that of RT55 4 wt% and RT55 10 wt% samples but using a mixture of RT55:RT70HC (90:10 wt%) instead of only RT55. These samples, thereafter named RT55N 4 wt% and RT55N 10 wt%, aimed at reducing the undercooling effect of the nano-encapsulated RT55 by adding a small amount of the PCM melting at higher temperature.

Moreover, SWCNHs (provided by Carbonium S.r.l.) were tested in the RT70HC 4wt% emulsion with the two-fold purpose of reducing the undercooling effect, acting as nucleating agent, and of modifying the optical properties of nano-emulsion, producing a black fluid. Four samples (namely NH1, NH2, NH3 and NH4) were prepared following different routes. Sample NH1 was prepared by dispersing 0.002 wt% of SWCNHs, with respect to the final weight of nano-emulsion, into the SDS/water solution and then following the previous preparation route; sample NH2 was prepared by dispersing 0.002 wt% of SWCNHs into the paraffin/hexane solution; sample NH3 was prepared in the same way as NH2 but a final concentration of 0.01 wt% SWCNHs was obtained; finally, NH4 was obtained by adding 0.002 wt% of SWCNHs after the preparation of nano-emulsion, by mixing it with an appropriate amount of pre-dispersed SWCNHs into a SDS/water solution. In fact, the different choice of dispersing SWCNHs either into the hexane solution or into the water solution aimed at investigating the influence of the carbon nanomaterial into the oil phase or the water phase, respectively. All the SWCNH suspensions were obtained by sonication with the Sonics VCX130 operated at 20 kHz and 65 W for 10 min.

A Malvern Zetasizer Nano ZS based on dynamic light scattering (DLS) technique was used for the evaluation of particles size distribution within the colloids and ζ-potential. Samples were observed using a TEM Philips CM12 operated at 120 kV and equipped with an energy dispersive X-ray spectrometer (EDXS). For TEM sample preparation the emulsions were diluted in distilled water and dispersed using an ultrasonic bath for 5 minutes. A drop of solution was put on a carbon coated TEM grid. The mean particle size was evaluated by means of ImageJ IJ 1.46r software. Thermal diffusivity measurements were carried out in the 30-70°C temperature range using a home-made device exploiting the photoacoustic effect. Details about the technique and device are reported elsewhere [21]. A Perkin-Elmer Lambda 35 UV–visible spectrophotometer equipped with a 1 mm quartz sample holder for liquids was used for the optical extinction characterization. A Differential Scanning Calorimeter (DSC, Setharam Instrumentation) was used to evaluate the melting/solidification temperatures and the associated enthalpy of fusion. The equipment is composed by two calorimetric cells in which three measurements are repeated. The first cell contains always an empty pot. The second cell contains an empty pot in the first measurement, a pot with a known reference material, sapphire, in the second measurement, and a pot with the emulsion in the third measurement. All the samples undergo to the same temperature variation of temperature, at the same velocity (2 or 3°C/min). A voltage signal, generated by the equipment, is measured as a function of temperature and velocity of temperature raising/decreasing. The instrument uncertainty is 2%. The viscosity of emulsions was measured by a rotational rheometer, AR G2, TA Instruments in the 0-1600 s^{-1} shear rate range. The results reported in Table 4 are the mean values of three measures taken at 755 s-1 of shear rate, while in Supplementary Information all the values are reported.

Table 1. Parameters for the preparation of 5g of nano-emulsions

Commercial name	Melting T	Latent Heat	Hexane	*Water*	PCM % in final emulsion	SDS % in final emulsion	Sonication T	Solvent evaporation conditions	
	(°C)	*(kJ/kg)*	*(g)*	*(g)*	*wt%*	*wt%*	*(°C)*	*(°C)*	*(h)*
RT55	55	140	1	5	2	0.25	RT	90	2
			1	5	4	0.5	45	90	2
			2.5	12.5	10	1.25	45	90	3
RT70HC	70	230	1	5	2	0.25	50	90	2
			1	5	4	0.5	60	90	2
			2.5	12.5	10	1.25	60	90	3

3. Results and discussion

Stable and homogeneous emulsions were achieved by this method. The pH of all emulsions ranged between 7.8 and 8.4. Figure 1 shows pictures of the nano-emulsions based on RT55 and RT70HC PCMs. In both cases, the 2 wt% and 4 wt% samples appeared translucent and transparent, qualitatively indicating a good emulsion with relatively small oil phase droplet size (around 100 nm), while the 10 wt% samples are more opaque and white, due to the higher concentration and, as reported hereafter, bigger size of PCM phase.

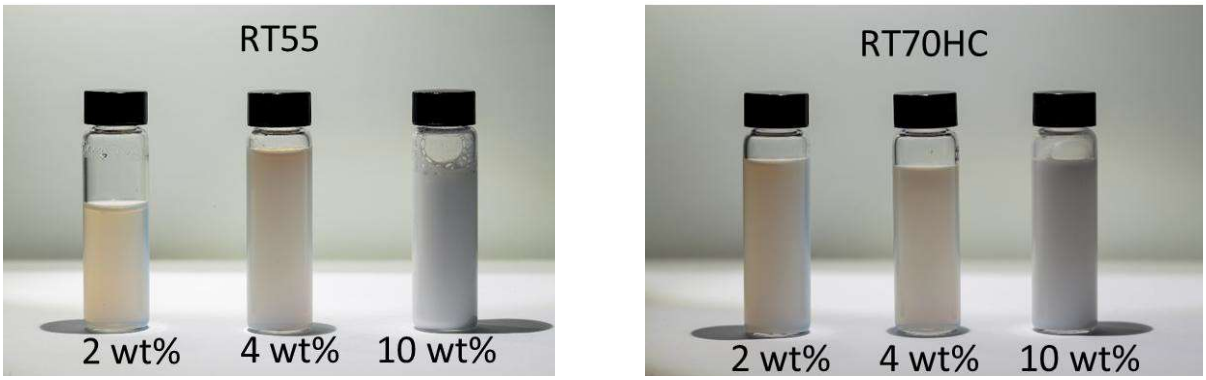

Figure 1. Pictures of the base nano-emulsions.

Table 2. DLS hydrodynamic size and ζ-potential measurements of base nanoemulsions.

Sample	**Mass concentration in final emulsion**	**Average size**	**ζ-potential**
	wt%	*(nm)*	*(mV)*
RT55	2	91	-104
	4	83	-74
	10	177	-68
RT70HC	2	65	-67
	4	110	-57
	10	223	-46

In fact, as reported in table 2, DLS measurements showed average sizes below 100 nm for samples RT55 2 wt%, RT55 4 wt%, RT70HC 2 wt% and slightly higher for sample RT70HC 4 wt%. Conversely, 10 wt% samples showed 177 nm and 223 nm for sample RT55 and RT70HC, respectively. TEM analyses revealed that the paraffin nucleus of the droplets is smaller, being for example of about 30-40 nm for RT55 4wt% and 45-55 nm for RT70HC 4wt%, as shown in figure 2. The difference in size is probably due to SDS shell, which most likely is the halo observed in TEM analyses around the particles.

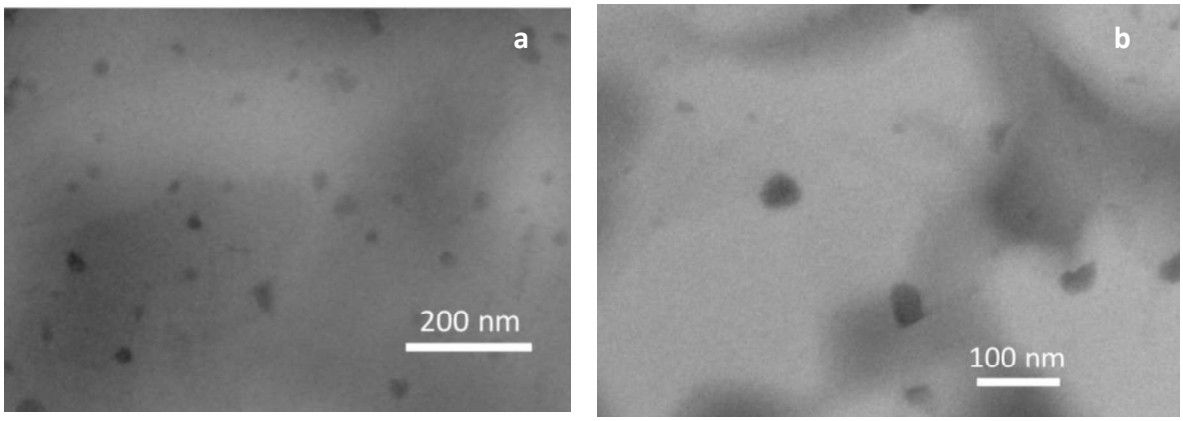

Figure 2. TEM analyses of PCME with a) RT55 4wt% and b) RT70HC 4wt%.

ζ-potentials, reported in table 2, were very high in absolute value for all samples, suggesting a good colloidal stability, with values decreasing with PCM concentration. The reduction of ζ-potential reflects on the particle size, which increases with paraffin concentration. These results show the efficacy of the proposed method of preparation, that is able to provide emulsions of PCMs with average droplet sizes around 100 nm, for concentrations up to 10 wt%. The visual inspection of all emulsions verified the stability for several months. DLS analyses were also performed for 30 days after few freeze-thaw cycles and found values similar to those reported in table 2 and with very low variance for all emulsions. As an example, sample RT55 2 wt% was thermally cycled 10 times between 25 and 65°C and DLS measurements repeated after that for 30 days showed a mean size of 91 nm with a ± 1 nm deviation within the entire moth (see Figure S1 in Supplementary Information). The emulsion with 2 wt% of RT55 was also kept for 2 days at temperatures ranging between 80 and 100°C while magnetically stirred at 1000 rpm. After this test the emulsion was visually unchanged (see Figure S2 in Supplementary Information) and the DLS revealed a mean size of 75 nm, with a slightly higher poly-dispersity. This indicated that, even if the particles size slightly changed, no significant aggregation nor sedimentation occurred.

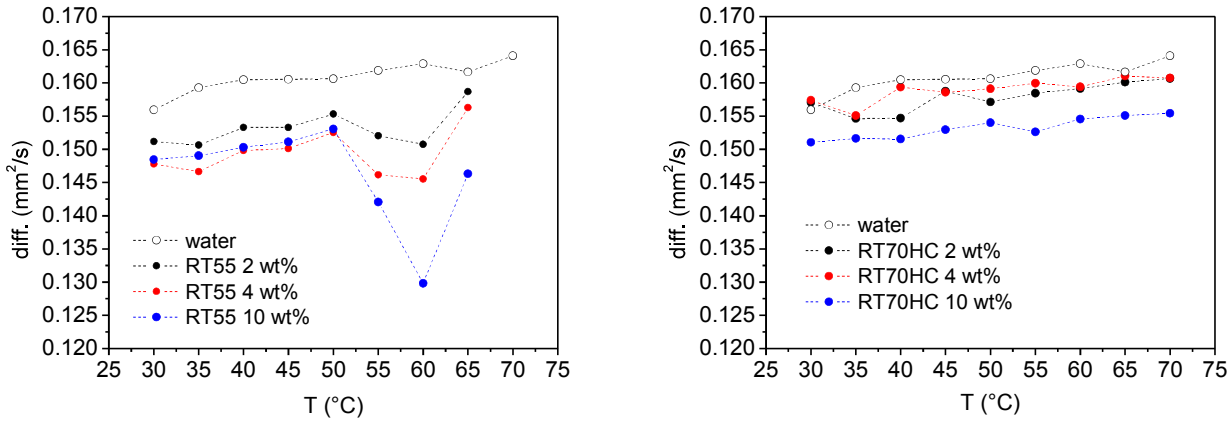

Figure 3. Thermal diffusivity of RT55 (a) and RT70HC (b) emulsions.

Figure 3 shows thermal diffusivity measurements obtained with a photoacoustic device in the 30-70°C range for the nano-emulsions, compared to deionised water. In the case of RT55 samples, the measurements seem affected by the melting process of PCM. In fact, the main feature of figure 2(a) is a reduction of thermal diffusivity starting at nominal melting point of PCM (55°C), with a minimum at around 60°C. The effect disappears with the completion of melting process and is more evident with increasing concentration. The effect is not visible for the RT70HC samples, whose melting start at around 70°C. The effect is probably explained by an artefact related to the measurement method. In fact, the measurement is partially based on the attenuation of the intensity of thermal waves produced by a modulated laser impinging on the top of the sample and traveling through it toward an acoustic cavity. Around the melting point of PCM, the thermal waves traveling through the sample are over attenuated by the transition, resulting in the observed effect. Excluding this region, that evidently underestimates the thermal diffusivity, all the samples showed a reduction of diffusivity with respect to pure water, due to the lower thermal diffusivity of PCM. The reduction is obviously higher by increasing concentration. However, while the reduction is about 6.3 % for RT55 PCM with a concentration of 10 wt%, the reduction is only 4.7 % for RT70HC 10 wt% sample. The difference in thermal diffusivity reduction is probably due to a difference in composition of RT55 and RT70HC.

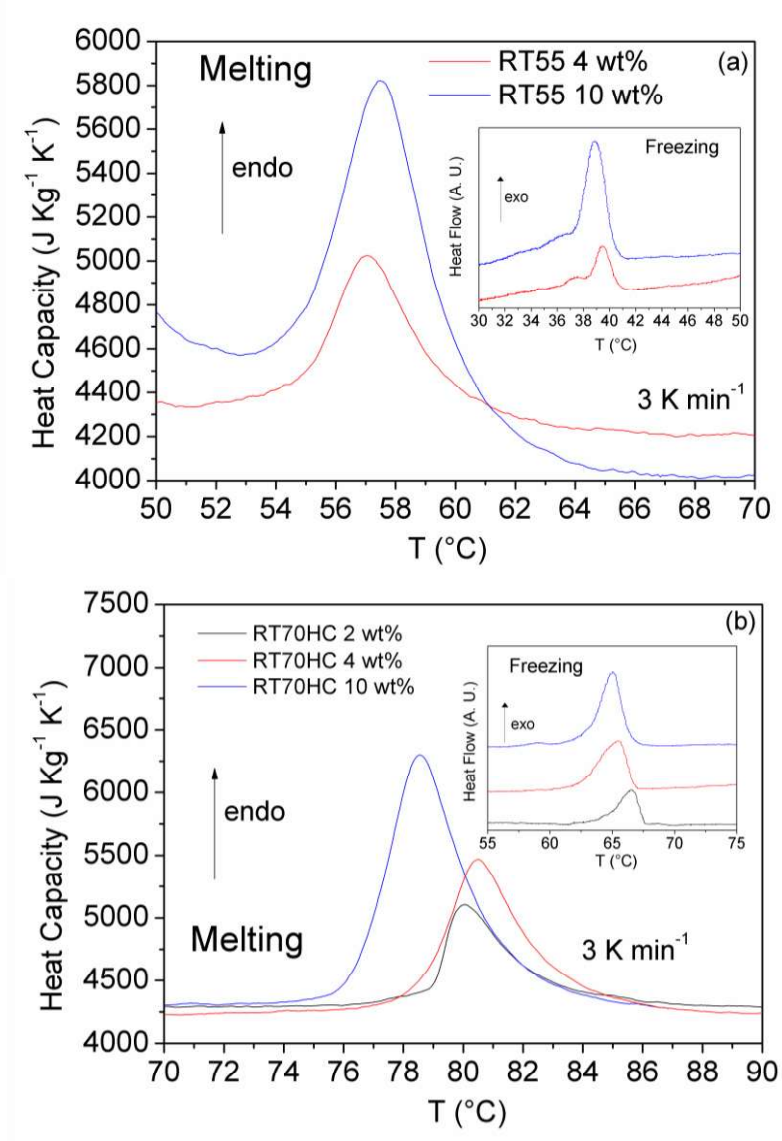

Figure 4. DSC melting curves of RT55 (a) and RT70HC (b) nano-emulsions (insets contain freezing curves).

DSC measurements were performed on all nano-emulsions, but the measurement on sample RT55 2 wt% did not provide useful information due to the low signal-to-noise ratio. The measured profiles reported in figure 4 show endothermic peaks whose intensity depends on PCM content. As already shown by other authors [9], emulsions of paraffin in water show an undercooling effect that could be detrimental for practical applications. The results are summarized in table 3. With respect to bulk material, the undercooling is about 16°C for RT55 samples and 10-11°C for RT70HC samples. The temperature onset of melting is compatible with the nominal values for samples RT55 but it is higher for samples RT70HC, with a melting temperature shift of about 6-9°C. A shift to higher melting was already observed by Huang L. et al [9] for Rubitherm paraffin, and was attributed to a difficulty in defining the melting temperature by using the onset point in mixtures as Rubitherm products. We can suppose that in such commercial PCM mixtures, any even negligible difference in melting temperatures of the components of the commercial products in bulk can be highlighted in case of nanoparticles, where a difference in composition and in melting temperatures can enlarge the curves. A further hypothesis is that SDS induces an interface thermal resistance that could delay/interfere with the melting process.

Table 3. DSC measurements results of base nano-emulsions.

Sample	**PCM mass concentration in emulsion**	**Melting *T***	**Solidification *T***	**Heat of melting**	**Expected Heat of melting**	**Difference**
	wt%	*(°C)*	*(°C)*	*(J kg^{-1})*	*(J kg^{-1})*	*(%)*
RT55	4	54.7	40.3	2758	5600	-50.7
	10	54.9	40.7	5180	14000	-63.0
RT70HC	2	78.9	67.6	2601	4600	-43.4
	4	78.5	66.8	4586	9200	-50.1
	10	76.4	66.5	7568	23000	-67.1

The main difference with respect to what is reported for the bulk materials is the lower heat of melting. The measured latent heats for the emulsions are about 40%, up to about 67%, lower with respect to the values estimated from the heat of melting of bulk paraffin and the PCM mass fraction in the emulsion. This was already observed in n-octacosane-in-water emulsions [12] and could be due to the PCM molecules on the surface of the nanoparticles that are anchored to the surfactant and this could delay or suppress their fusion. However, if we calculate the thermal capacity increase of PCME with respect to pure water from measured data (see Figure 5) calculated as:

$$\Delta H_{\%} = 100\left(\frac{\left(X_{PCM}c_{P_{PCM}} + (1 - X_{PCM})c_{p_{water}}\right)\Delta T + L_{PCME}}{c_{p_{water}}\Delta T} - 1\right)$$

Where X_{PCM} is the weight fraction of PCM, $c_{P_{PCM}}$ and $c_{p_{water}}$ are the specific heats of PCM and water respectively, L_{PCME} is the measured latent heat of phase change of PCM emulsion and ΔT is the

temperature difference between the cold and hot sides of a hypothetical heat exchange device around the phase change temperature, we observe that we can have a gain in storage heat capacity even up to a 40% for a ΔT of 4°C. As can be seen in Figure 5, the enhancements increase with increasing concentration and are higher for RT70HC emulsions. As observed in Figure 5, this increase is nevertheless limited to working temperatures close to the melting temperatures of PCM (within 20-30°C) since the specific heat capacity of PCM is lower than that of water. It is nonetheless worth highlighting that the preparation of PCME could allow the use of multiple PCMs with different melting temperatures in the same emulsion thus expanding the possible operating temperature range.

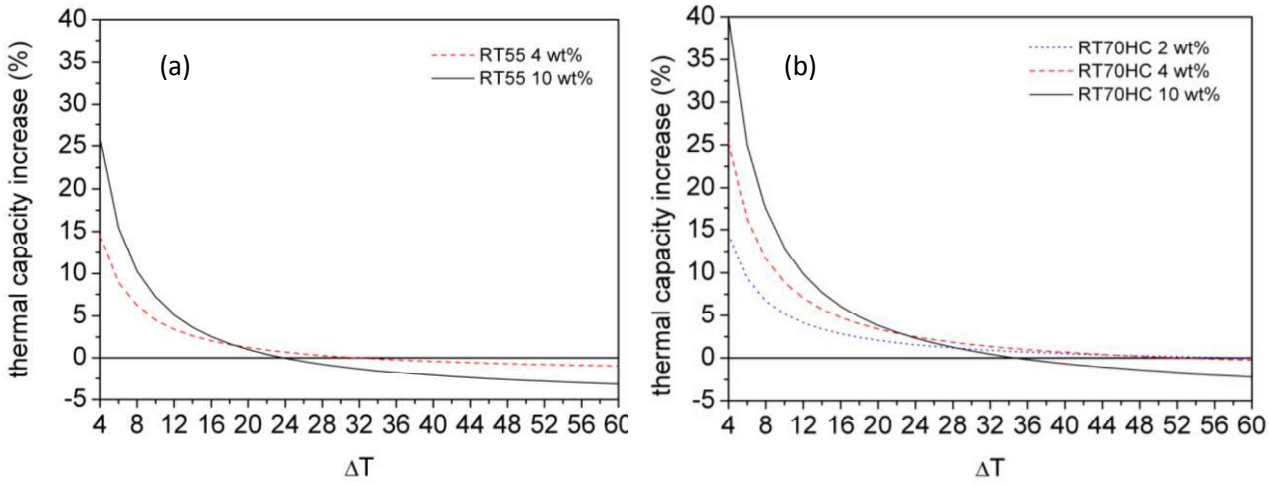

Figure 5. Thermal capacity increase of PCME with respect to pure water, reported as a function of ΔT from the melting temperatures and calculated from DSC measured data, for a) RT55 and b) RT70HC based emulsions.

The viscosity of emulsions was measured and the results reported in Table 4 and Figure S3 in Supplementary Information. The viscosity increased as expected with concentration, but the increase was moderate for concentrations up to 4wt%, while was high for higher concentration, showing a non-Newtonian behaviour for the RT70HC 10wt% sample. Considering an increase of thermal capacity of about 15-25% for the emulsions with 4wt%, for practical applications the concentration could be limited to this value.

Table 4. Mean viscosity results of RT55 and RT70HC nano-emulsions.

Sample		Viscosity (Pa s)	μ_{PCME}/μ_{water}
Water (Refprop)		8.90×10^{-4}	1
RT55	2 wt%	9.64×10^{-4}	1.08
	4 wt%	1.28×10^{-3}	1.44
	10 wt%	3.87×10^{-3}	4.35
RT70HC	2 wt%	1.22×10^{-3}	1.37
	4 wt%	1.66×10^{-3}	1.87
	10 wt%	4.55×10^{-3}	5.11

To decrease the undercooling effect, RT70HC was added as nucleating agent to RT55. Table 5 reports the DLS and ζ-potential results of RT55N samples, prepared by dissolving a mixture of RT55 (90 wt%) and RT70HC (10 wt%) into hexane. The results, compared with those of the homologous RT55 samples, show

that the droplet size and the ζ-potential are substantially unvaried for the mixture, but the melting onset temperatures were lowered from 55°C to 49°C and the solidification temperatures increased from 40°C to 47°C, reducing the undercooling to 2°C. The emulsions were stable over time and after freeze-thaw cycle, as observed in Figure S1.

Table 5. DLS, ζ-potential and DSC results comparison between RT55 and RT55N samples.

% RT55	**% RT70HC**	**average size**	**ζ-potential**	**Melting *T***	**Solidification T**	**Undercooling**
wt%	*wt%*	*(nm)*	*(mV)*	*(°C)*	*(°C)*	*(°C)*
4		83	-74	54.7	40.3	14.4
3.6	0.4	96	-79	49.0	46.7	2.3
10		177	-68	54.9	40.7	14.2
9	1	173	-66	49.1	46.5	2.6

The DSC heating profiles of the two samples are reported in figure 6. The heats of melting estimated from the area under the peaks are anyway further reduced with respect to RT55 samples, 28% less with respect to sample RT55 4 wt% and about 30% with respect sample RT55 10 wt%.

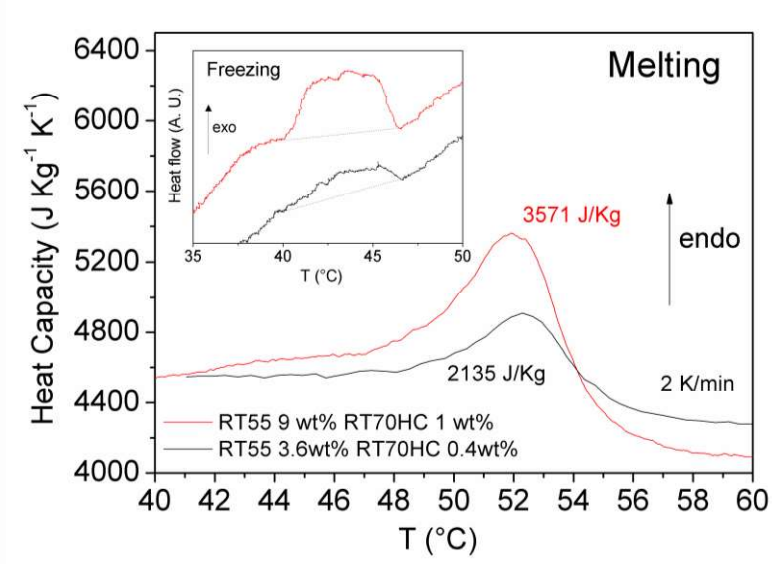

Figure 6. DSC heating profiles of RT55N nanoemulsions (cooling curves in inset).

Therefore, the RT70HC was successful in reducing the melting/solidification undercooling but with a reduction on latent heat. A particular carbon nanostructure was also investigated in RT70HC 4% emulsion with the double objective of testing it as nucleating agent and increasing the optical absorption of the fluid in order to evaluate the volumetric solar absorption capacity of the resulting fluids. Figure 7 shows the appearance of samples containing SWCNHs, both prepared with SWCNHs dispersed into the water or in hexane solutions. Even if samples NH1 and NH2 and NH4 show both a blue-grey colour, a slight difference is not appreciable in the picture, while sample NH1 is discernibly more whitish. Sample NH3, due to higher concentration of SWCNHs, looks very black.

Figure 7. Nano-emulsions based on RT70HC 4wt% containing SWCNHs.

Sample NH3 was characterized by DLS for the estimation of droplets hydrodynamic size and ζ-potential and DSC to study the effect of SWCNHs on the melting and solidification temperatures of PCM. The results reported in table 6 show that the droplet size is 50 % bigger than the homologous sample not containing SWCNHs, and this is the result that is expected if SWCNHs are incorporated into the PCM phase. ζ-potential is also bigger in absolute value, which is probably due to the charged functional groups naturally present on the surface of the carbon nanomaterial [22].

Table 6. Effect of the presence of SWCNHs on DLS and DSC results.

% RT70HC	**% SWCNHs**	**Average Size**	**ζ-potential**	**Melting *T***	**Solidification *T***	**Undercooling**
wt%	*wt%*	*(nm)*	*(mV)*	*(°C)*	*(°C)*	*(°C)*
4		110	-57	78.5	66.8	11.7
4	0.01	166	-68	73.3	66.6	6.7

As previously observed, sample RT70HC 4 wt% shows a slightly higher melting point with respect to the nominal value (78°C vs. 70°C) and a solidification at 67°C. While the latter seems not to be affected by the presence of SWCNHs, the melting point is lowered towards the nominal value at 73°C, resulting in a temperature difference of about 7°C between melting and solidification. The effect can be explained by a more efficient heat transfer between water and the PCM phase due to the higher thermal conductivity of carbon nanomaterial that are into intimate contact.

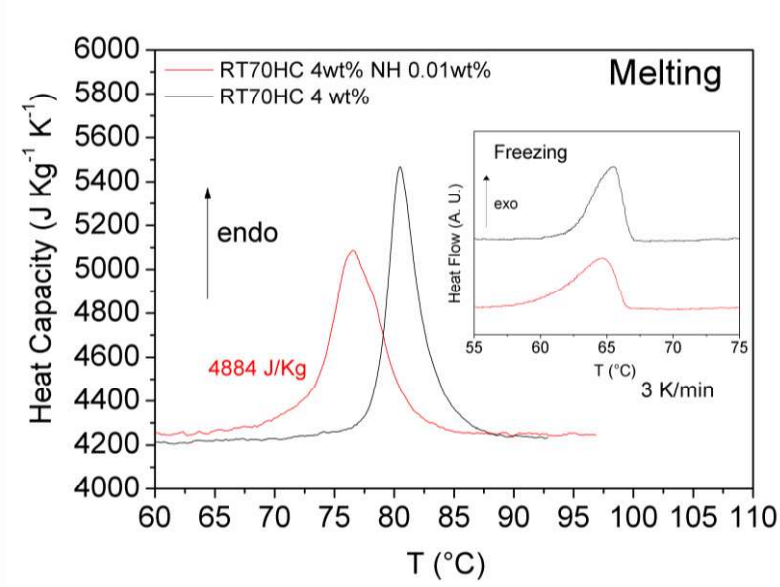

Figure 8. DSC heating profile of NH3 nano-emulsion compared with RT70HC 4 wt% (cooling curves in inset).

The heating and cooling DSC profiles of sample NH3 are reported in figure 8. The melting peak of NH3 is broader with respect to that of RT70HC 4 wt%, but the heat of melting is slightly higher (about 6 %).

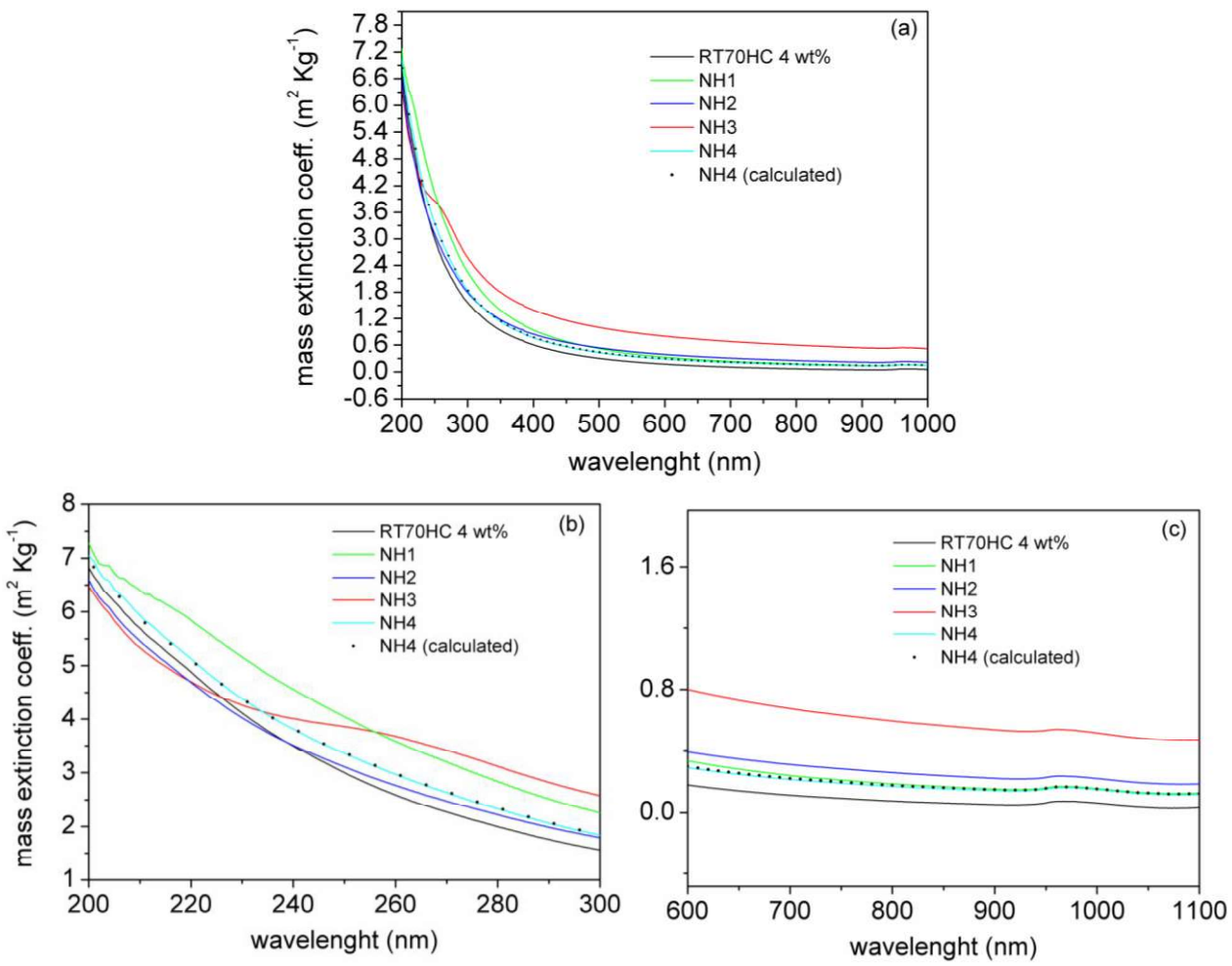

Figure 9. UV- Vis mass extinction coefficient of RT70HC 4wt% samples containing SWCNHs (a), detail in the wavelength range 200 - 300 nm (b) and in the range 600 - 1100 nm (c).

To test the optical volumetric absorption capabilities of these emulsions, UV-Vis measurements were performed. Figure 9 (a) shows a comparison of UV-Vis mass extinction coefficient of sample RT70HC 4 wt% samples NH1, NH2, NH3, NH4 and a theoretical spectrum for the RT70HC 4 wt% + 0.002 wt% SWCNHs calculated from the experimental spectra of RT70HC 4 wt% and that of a SWCNHs suspension in water. Observing figure 9 (c), the detail of the spectra from 600 nm to 1100 nm, which is the part less affected by scattering, sample NH3 obviously shows the maximum absorption due to the higher content of SWCNHs with respect to other samples. Samples NH1 and NH4 overlap the calculated spectrum corresponding to the simple mixing of SWCNHs suspension and RT70HC 4 wt%. The situation is quite different in the 200 – 300 nm, where the effect of scattering is prevailing. Sample NH3 shows a shoulder at 260 nm that corresponds to the π-π^* plasmonic peak of SWCNHs [22], while at the shortest wavelengths the mass extinction coefficient is lower than all other samples, meaning a much lower light scattering. In a consistent manner, sample NH2, which also should contain SWCNHs into the PCM phase, shows a lower scattering with respect to the other samples where SWNHs are into the water phase. Sample NH1 shows the highest mass extinction coefficient in the shorter wavelength region that means a higher scattering. Sample NH4 follows exactly the theoretical behaviour corresponding to the simple mixing of components. Therefore, it seems that introducing SWCNHs in the hexane during synthesis resulted in having the higher absorption among the nano-emulsions tested and reduced also the scattering due to PCM nanoparticles.

4. Conclusions

A new solvent-assisted route was developed to produce nano-emulsions of commercial paraffin waxes in water. Concentrations from 2 to 10 wt% were obtained starting from two commercial paraffin waxes, with nominal melting temperatures of 55°C and 70°C. The paraffin and paraffin/surfactant particle dimensions were verified by DLS and TEM and by paraffin/surfactant sizes resulted below 100 nm for lower concentrations and slightly higher for 10 wt%. The stability of emulsions was verified by long-term tests, freeze-thaw cycles and by keeping the emulsions at 1000 rpm and a temperature higher than the melting point for 2 days. The viscosity increase was moderate for emulsions up tp 4wt%.

The melting and crystallization temperatures as well as the latent heat were measured by DSC. An undercooling effect, typical of emulsions, was verified and strongly reduced to about only 2°C by the addition of 10% of the paraffin melting at 70°C to the paraffin melting at 55°C. The heat of melting of emulsions is lower with respect to the expected values, from about 40% up to about 67%. This may be due to the PCM molecules on the surface of the nanoparticles that are anchored to the surfactant and this could delay or suppress their fusion. However, if we calculate the thermal capacity increase of PCMEs with respect to pure water from measured data, we observe a gain in storage heat capacity even up to a 40%. The thermal capacity increases with increasing concentration and is higher for RT70HC emulsions. This gain is limited to working temperatures close to the melting temperatures of PCM (within 20-30°C). It is nonetheless worth highlighting that the preparation of PCME could allow the use of multiple PCMs with different melting temperatures in the same emulsion thus expanding the possible operating temperature range.

The thermal diffusivity was measured and resulted slightly lower than the water thermal diffusivity. Moreover, it decreases with increasing concentration, as expected due to the lower thermal diffusivity of paraffin. Optical measurements of SWCNH/paraffin composites indicated that introducing SWCNHs in the hexane during synthesis resulted in having the higher absorption among the nano-emulsions tested and a reduced scattering due to PCM nanoparticles.

References

[1] European Commission, An EU Strategy on Heating and Cooling, SWD2016 (2016) https://ec.europa.eu/energy/sites/ener/files/documents/1_EN_ACT_part1_v14.pdf

[2] http://ec.europa.eu/eurostat/statistics-explained/index.php/Renewable_energy_statistics (accessed June 2018)

[3] J. Shao, J. Darkwa, G. Kokogiannakis, *Review of phase change emulsions (PCMEs) and their applications in HVAC systems,* Review Energ. Build. 94 (2015) 200-217.

[4] M. Hany Abokersh, M. Osman, O. El-Baz, M. El-Morsi, O. Sharaf, *Review of the phase change material (PCM) usage for solar domestic water heating systems (SDWHS)*, Int. J. Energy Res. 42 (2018) 329

[5] Z. Qiu, X. Ma, P. Li, X. Zhao, A. Wright, *Micro-encapsulated phase change material (MPCM) slurries: Characterization and building applications*, Renew. Sust. Energ. Rev. 77 (2017) 246–262

[6] V. Mikkola, S. Puupponen, K. Saari, T. Ala-Nissila, A. Seppala, *Thermal properties and convective heat transfer of phase changing paraffin nanofluids*, Int. J. Thermal Sci. 117 (2017) 163-171.

[7] S. Puupponen, A. Seppala, O. Vartia, K. Saari, T. Ala-Nissila, *Preparation of paraffin and fatty acid phase changing nanoemulsions for heat transfer*, Thermochim. Acta 601 (2015) 33-38.

[8] C. Liu, Z. Rao, J. Zhao, Y. Huo, Y. Li, *Review on nanoencapsulated phase change materials: Preparation, characterization and heat transfer enhancement*, Nano Energy 13 (2015) 814-826.

[9] L. Huang, E. Günther, C. Doetsch, H. Mehling, *Subcooling in PCM emulsions—Part 1: Experimental*, Thermochim. Acta 509 (2010) 93.

[10] M. Delgado, A. Lázaro, J. Mazo, B. Zalba, *Review on phase change material emulsions and microencapsulated phase change material slurries: Materials, heat transfer studies and applications*, Renew. Sust. Energ. Rev. 16 (2012) 253– 273.

[11] J. Chen, P. Zhang, *Preparation and characterization of nano-sized phase change emulsions as thermal energy storage and transport media*, Appl. Energy 190 (2017) 868–879.

[12] X. Zhang, J. Wu, J. Niu, *PCM-in-water emulsion for solar thermal applications: The effects of emulsifiers and emulsification conditions on thermal performance, stability and rheology characteristics*, Sol. Energ. Mat. Sol. Cells 147 (2016) 211–224.

[13] L. Yu, C. Li, J. Xu, J. Hao, D. Sun, *Highly Stable Concentrated Nanoemulsions by the Phase Inversion Composition Method at Elevated Temperature*, Langmuir, 28 (2012) 14547-14552.

[14] E. Günther, L. Huang, H. Mehling, C. Dötsch, *Subcooling in PCM emulsions – Part 2: Interpretation in terms of nucleation theory*, Thermochim. Acta 522 (2011) 199–204.

[15] S. Zhang, J.Y. Wu, C. Tse, J. Niu, *Effective dispersion of multi-wall carbon nano-tubes in hexadecane through physiochemical modification and decrease of supercooling*, Sol. Energ. Mat. Sol. Cells 96 (2012) 124.

[16] Z. Wang, F. Qiu, W. Yang, X. Zhao, *Applications of solar water heating system with phase change material*, Renew. Sust. Energ. Rev. 52 (2015) 645

[17] T. P. Otanicar, P. E. Phelan, J. S. Golden, Optical properties of liquids for direct absorption solar thermal *energy systems*, Sol. Energ., 83 (2009) 969.

[18] E. Sani, S. Barison, C. Pagura, L. Mercatelli, P. Sansoni, D. Fontani, D. Jafrancesco, F. Francini, *Carbon nanohorns-based nanofluids as direct sunlight absorbers*, Opt. Express, 18 (2010) 5179

[19] A.H. Elsheikh, S.W. Sharshir, M.E. Mostafa, F.A. Essa, M.K. Ahmed Ali, *Applications of nanofluids in solar energy: A review of recent advances*, Renew. Sust. Energ. Rev. 82 (2018) 3483.

[20] A. Kasaeian, A. Toghi Eshghi, M. Sameti, *A review on the applications of nanofluids in solar energy systems*, Renew. Sust. Energ. Rev. 43 (2015) 584.

[21] F. Agresti, A. Ferrario, S. Boldrini, A. Miozzo, F. Montagner, S. Barison, C. Pagura, M. Fabrizio, *Temperature controlled photoacoustic device for thermal diffusivity measurements of liquids and nanofluids*, Thermochim. Acta, 619 (2015) 48-52.

[22] F. Agresti, S. Barison, A. Famengo, C. Pagura, L. Fedele, S. Rossi, S. Bobbo, M. Rancan, M. Fabrizio, *Surface oxidation of Single Wall Carbon Nanohorns for the production of surfactant free water-based colloids*, J. Colloid Interf. Sci. 514 (2018) 528-533.